Differentiation for High-Precision GPS Velocity and Acceleration Determination

A.M. BRUTON, C.L. GLENNIE, and K.P. SCHWARZ *Department of Geomatics Engineering, The University of Calgary, Alberta, Canada*

Accurate estimates of the velocity and acceleration of a platform are often needed in high dynamic positioning, airborne gravimetry, and geophysics. In turn, differentiation of GPS signals is a crucial process for obtaining these estimates. It is important in the measurement domain where, for example, the phase measurements are used along with their instantaneous derivative (Doppler) to estimate position and velocity. It is also important in postprocessing, where acceleration is usually estimated by differentiating estimates of position and velocity. Various methods of differentiating a signal can have very different effects on the resulting derivative, and their suitability varies from situation to situation. These comments set the stage for the investigations in this article. The objective is twofold: (1) to carry out a comprehensive study of possible differentiation methods, characterizing each in the frequency domain; and (2) to use real data to demonstrate each of these methods in both the measurement and position domains, in conditions of variable, high, or unknown dynamics. Examples are given using real GPS data in both the measurement domain and in the position and velocity domain. The appropriate differentiator is used in several cases of varying dynamics to derive a Doppler signal from carrier phase measurements (rather than using the raw Doppler generated by the receiver). In the static case, it is seen that the accuracy of velocity estimates can be improved from 4.0 mm/s to 0.7 mm/s by using the correct filter. In conditions of medium dynamics experienced in an airborne gravity survey, it is demonstrated that accelerations at the 2–4 mGal level (1 mGal = 0.00001 m/s^2) can be obtained at the required filtering periods. Finally, a precision motion table is used to show that when using the correct filter, velocity estimates under high dynamics can be improved by an order of magnitude to 27.0 mm/s. © *1999 John Wiley & Sons, Inc.*

GPS Solutions, Vol. 2, No. 4, pp. 7–21 (1999)

CCC 1080-5370/99/040007-15

INTRODUCTION

The differentiation of discrete-time signals in GPS has been frequently studied for velocity determination. In the measurement domain, investigations have been carried out to derive a Doppler by differentiating the carrier phase measurements rather than using the Doppler generated by the receiver. This approach has been considered advantageous because the resulting Doppler is less noisy than the raw Doppler. Several methods of differentiation have been investigated for this purpose. Fenton and Townsend (1994) demonstrated the use of parabolic functions. Both Cannon et al. (1997) and Hebert (1997) approached this task using simulated GPS data by applying low-order Taylor series approximations of the derivative and by differentiating cubic spline fits. A Kalman filter approach was also proposed and applied by Hebert (1997). In each of these cases, good solutions were observed in static and low dynamic cases, but errors increased with higher dynamics.

Several investigations have also been made into determining acceleration by differentiating position and velocity. Consider, for example, the following studies of acceleration determination for airborne gravimetry: Brozena et al. (1989), Wei et al. (1991), and Van Dierendonck et al. (1994). However, little work has been done in considering different methods of differentiating these signals, especially in cases that are not band limited.

To evaluate and compare different methods of dif-

ferentiation, the concept of an ideal differentiator will be described in Section 1. This will be used along with the frequency responses of each method to characterize their response to different vehicle dynamics. The use of low-order Taylor series approximations of the derivative will first be studied. Design of differentiating filters using the Fourier series method will then be treated. For this approach, it will be shown that important errors in the resulting responses can be reduced using a window technique. The concepts of numerical and optimal design of differentiating filters will also be presented. It will be shown that these types of filters are required when differentiating signals for conditions of variable, high, or unknown dynamics.

Additionally, because it is intuitively pleasing to estimate the derivative by fitting a curve to the signal and differentiating it, least-squares polynomial fits will be considered in detail. It is obvious that in addition to differentiating the signal, such a fit offers a certain level of smoothing that is a function of parameters such as polynomial order and the length of the window in which the fit is made. The problem of fitting curves to the data will be reformulated so that the least-squares adjustment becomes a simple time domain convolution. Using this knowledge, the behavior of best-fit polynomials for differentiation is characterized as a function of both polynomial order and window length, and their ranges of applicability are quantified in terms of effective frequency range.

To bridge the gap between theory and application, the practical implementation of each of these differentiators will be discussed in Section 2. It will be shown that each method can be applied to real GPS data using a discrete time convolution. In other words, they can all be considered as nonrecursive or finite impulse response (FIR) filters. Issues of phase response and filter order will also be discussed.

Several examples using real GPS data will then be given in Section 3 to demonstrate the effectiveness and limitations of these filters for determining vehicle velocity and acceleration under different dynamic conditions. First, differentiation of signals in the measurement domain will be treated. A preprocessor has been developed that derives a Doppler by differentiating carrier phase measurements using any of the above-mentioned differentiators. Several methods will then be applied to three cases of increasing dynamics, namely, a static baseline, an airborne gravimetry survey, and data collected on a precision motion table. In the latter two cases, verification of results is accomplished using an independent reference, i.e., the known gravity field and a precise reference trajectory, respectively. Differentiation of signals in the position and velocity domains will then be considered in Section 4. The precise motion table will be used to determine the accuracy with which velocity can be determined from position, and the airborne gravity case will again be used to determine the accuracy of acceleration estimates derived from velocity. Finally, some conclusions and recommendations for future research will be presented.

1. PROBLEM STATEMENT AND ANALYSIS

In this section, the problem of estimating the derivative of a discrete time signal will be treated in detail. Various methods of differentiation will be analyzed, leading to discussions about their suitability in different situations. The concept of an ideal digital differentiator is described and will be used to characterize the behavior of each differentiator in the frequency domain, or as a function of different vehicle dynamics. After this, the discussion proceeds by analyzing each of the proposed methods of differentiation in the frequency domain. The methods investigated are the low-order Taylor series approximations, designs based on the Fourier series and window techniques, numerical designs, optimal designs, and finally the differentiation of polynomial and spline fits. The results of these analyses will be used in Section 2 to develop effective methods of deriving Doppler and estimating velocity and acceleration from position and velocity estimates, respectively.

1.1. The ideal differentiator

To differentiate a discrete time signal, what is needed is a discrete time system that, when applied to input samples of a bandlimited continuous time signal, produces a sample of its derivative. Although it is impossible to design such a system exactly, consider what it might look like. The ideal digital differentiator can be written in the following form (from Antoniou, 1993, p. 303):

$$H(e^{j\omega T}) = j\omega \text{ for } 0 \leq |\omega| < \frac{\omega_s}{2} \tag{1}$$

where ω is the frequency, ω_s is the sampling frequency, and T is the corresponding sampling period. The magnitude of the frequency response of this system is shown as the dotted line in Figure 1. Our goal in deriv-

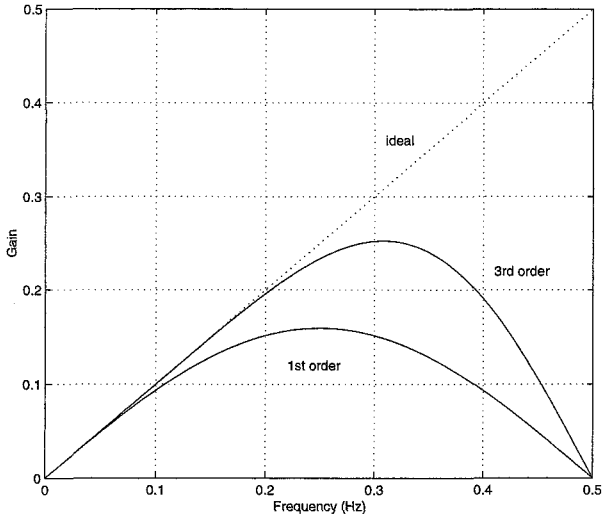

FIGURE 1. Magnitude response of the ideal differentiator and two low-order Taylor series approximations.

ing Doppler measurements, for example, can therefore be seen as approximating this idealization and applying it to the phase measurements. It will be used later to assess the quality of each of the differentiators proposed.

1.2. Design and implementation of differentiators

In GPS systems, the application of digital filters is restricted by several important practical considerations. As will be seen, many of these considerations are dealt with by using FIR filters. This is mainly done because of the ease of filter implementation. Practically, an FIR differentiator can be applied to a discrete data set $x(t)$ using a convolution as follows:

$$x'(t) = \sum_{k=0}^{N-1} h(k)x(t-k) \tag{2}$$

where $x'(t)$ is the derivative of the input signal $x(t)$ at time t, and h is the impulse response with order $(N-1)$ corresponding to the differentiator H. Theoretically, the relationship between the impulse response h and the ideal digital differentiator in Eq. (1) is given by

$$h(nT) = \frac{1}{\omega_s} \int_{-\omega_s/2}^{\omega_s/2} H(e^{j\omega T}) e^{j\omega T} d\omega \tag{3}$$

Practically then, the design of a digital differentiator becomes the problem of designing an impulse response h that can be applied to a data set using Eq. (2) and that has a frequency response as close as possible to that in Eq. (1).

A second consideration is the high dependence of the output of the system on the temporal characteristics of the signals. If filters are designed to have a symmetric impulse response, a FIR filter has linear phase, meaning that only a constant time delay will be caused and easily corrected for, especially in postmission applications. A third consideration is the order of the filter, which is related to the length of the window in which a filter is applied. If a filter has to be reset because of unavoidable events, then errors caused by edge effects have to be dealt with. These errors will affect less data if the filter order is small. Cycle slips in GPS are a good example of such unavoidable events.

1.3. Low-order Taylor series approximations

Low-order Taylor series approximations obtained from the definition of the derivative of a continuous function are given as follows:

$$x'(t) = \lim_{\delta t \to 0} \frac{x(t+\delta t) - x(t)}{\delta t} \tag{4}$$

By using Taylor's Theorem, it can easily be shown (as in Cheney and Kincaid, 1994, pp. 151–153) that the first-order central difference approximation to this derivative is given by

$$x'(t) = \frac{x(t+\delta t) - x(t-\delta t)}{2\delta t} \tag{5}$$

In this way, the derivative of x at time t is estimated using data at two epochs (times $t+\delta t$ and $t-\delta t$). This is the first-order central difference approximation. Higher order central differences that use more data epochs to either side of time t can also be developed along these lines. The third-order central difference, for instance, is of the form

$$x'(t) = 45\frac{x(t+\delta t) - x(t-\delta t)}{60\delta t} - 9\frac{x(t+2\delta t) - x(t-2\delta t)}{60\delta t} + \frac{x(t+3\delta t) - x(t-3\delta t)}{60\delta t} \tag{6}$$

The first- and third-order differentiators given above have the following impulse responses:

$$h=\frac{1}{2}[1\ \ 0\ \ -1]^T \text{ and} \tag{7}$$

$$h=\frac{1}{60}[1\ \ -9\ \ 45\ \ 0\ \ -45\ \ 9\ \ -1]^T \tag{8}$$

and have amplitude responses as shown in Figure 1, assuming a sampling frequency ω_s of 1 Hz.

In examining Figure 1, a first observation is that the Taylor series are clearly good approximations of the ideal differentiator at low frequencies. The first-order approximation begins to deviate considerably from ideal at about 0.05 Hz and the third-order at about 0.15 Hz. This has several implications. First, if the signal being differentiated is primarily a very low-frequency signal, then either of these approximations may suffice. Second, if this is the case and there exists mainly noise in the upper part of the spectrum, then these differentiators will also serve to suppress that noise. Obviously, the applicability of these differentiators depends on the signal to be differentiated. Caution must be exercised if the signal of interest has medium- to high-frequency components because this type of differentiator will result in spectral distortion at mid to high frequencies, and ultimately in a derivative of poorer quality.

Investigations where low-order Taylor series approximations have been used in the GPS measurement domain include both Cannon et al. (1997) and Hebert (1997). Results verify the observations made above. The approximations worked well for static and low dynamic data sets but gave poor results for higher dynamics.

By increasing the order of the Taylor series approximation being used, better approximates of the ideal differentiator can be obtained, especially at low frequencies. This will be examined further in the discussion of numerical designs in Section 1.6.

1.4. Fourier Series design of differentiators

Equation 3 relates the impulse response h and the frequency response H of a differentiator and can be exploited to estimate the impulse response from the ideal response given in Eq. (1). Excellent discussions of this method are given in Antoniou, 1993 (p. 280) and Orfanidis (1996). This can be done in MATLAB™ using the IFFT function and by truncating and delaying the resulting impulse response. For a filter length of 25, this yields the differentiator shown in Figure 2. In the upper graph, the amplitude response of the filter and the ideal response are shown. In the lower graph, the error in the amplitude response is shown.

The oscillatory deviations of the filter from the ideal case in Figure 2 are commonly referred to as Gibbs' oscillations. These are caused by the discontinuity in $H(e^{j\omega T})$ at $\omega=\omega_s/2$ and can be reduced by using the window technique (Antoniou, 1993, p. 282). Essentially, this technique replaces the abrupt truncation of the impulse response by a gradual tapering that is defined by a window function. There are many window functions available. For example, the Blackman function is given by the following equation from Antoniou, 1993 (p. 290):

$$\omega(nT) = \begin{cases} 0.42 + 0.5\cos\dfrac{2\pi n}{N-1} + 0.08\cos\dfrac{4\pi n}{N-1} & \text{for } |n| \le \dfrac{N-1}{2} \\ 0 & \text{otherwise} \end{cases} \tag{9}$$

and illustrated in Figure 3a. Figure 3b and 3c show the impulse response h corresponding to the filter shown in Figure 2, before and after application of the Blackman window function with a cutoff frequency of $\omega_c = 0.4$ Hz. Clearly, the window function reduces the magnitude of the impulse response to either side of the center of the filter.

Figure 4 shows the corresponding effect on the am-

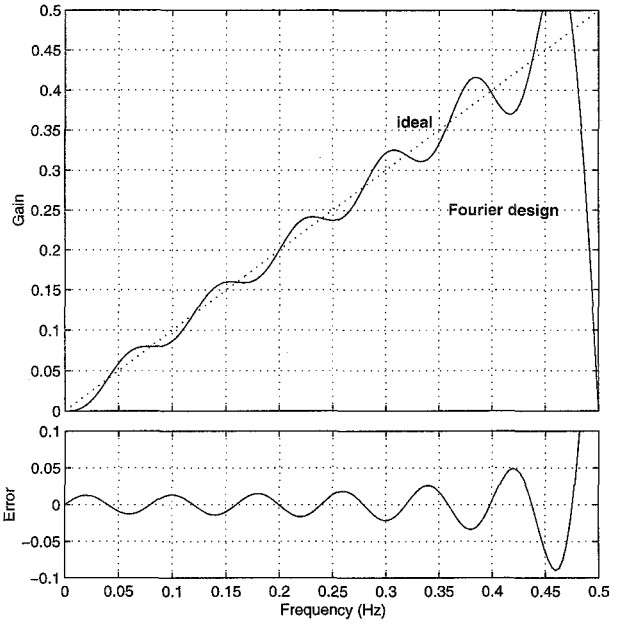

FIGURE 2. A 25th-order differentiator designed using the Fourier series.

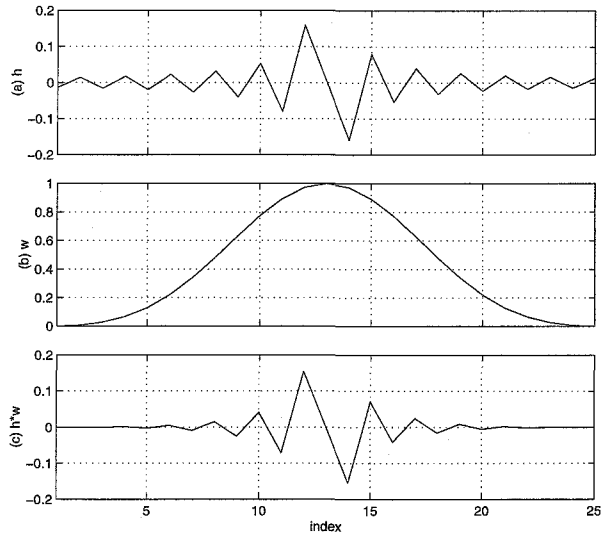

FIGURE 3. (a) Impulse response of the 25th-order Fourier series differentiator. (b) Blackman window. (c) Windowed impulse response.

plitude response of the filter. As in Figure 2, the upper graph shows the amplitude response of the filter and the ideal response, and the lower graph shows the error. The advantage of the window function is made clear by the reduction in the magnitude of Gibbs' oscillations. In examining Figures 2 and 4, it is clear that a window function can improve the amplitude response by several orders of magnitude. By using only symmetric window functions, the symmetry and therefore the linear phase properties of the filter are preserved. Examples of other window functions are given in Antoniou (1993, pp. 282–295) and Orfanidis (1996). Examples where window functions have been used in the design of filters for GPS-related research include Hammada (1996) and Skaloud and Schwarz (1998). In both cases, they were used for the design of low-pass filters.

On inspection of the magnitude response in Figure 4, it is clear that a differentiator that has been designed by using the Fourier series method will offer a good approximation of the ideal differentiator when a window function is used. It is also clear that such a filter has a wider range of applications than the low-order Taylor series approximations seen in Section 1.3 because it offers a better response over the whole frequency band. This has several implications. If the signal being differentiated has components at frequencies across the spectrum, then the output of the system will be a better approximation of the derivative. If noise only exists across a part of the spectrum, then the system will tend to amplify the noise. This is especially true if the signal of interest contains only low-frequency information.

By using larger filter orders, errors in the filter response can be decreased and the bandwidth of the filter can be increased. This is often undesirable, however, for instance, if the data are subject to unavoidable breaks such as cycle slips. A compromise must be reached between approximation error and tolerable filter order. This will depend on the application and will vary from situation to situation.

1.5. Optimal designs

Although no discrete-time system can be designed to perfectly match the ideal differentiator, FIR filters can be designed that very closely approximate it for all frequencies. In optimal design, the impulse response of the filter is obtained by minimizing the error in its amplitude response (with respect to the desired response) using optimization methods. In this article, we will use the Remez Exchange Algorithm as outlined in Antoniou, 1993 (pp. 578–586). Consider Figure 5, which shows the amplitude response of a 25th order differentiator designed using the Remez Exchange Algorithm provided in software accompanying Antoniou, 1993. The filter was designed so that it has a transition band between 0.4 and 0.5 Hz, ensuring no signal content above the Nyquist frequency, $\omega_s/2 = 0.5$ Hz, and therefore no aliasing of the signal.

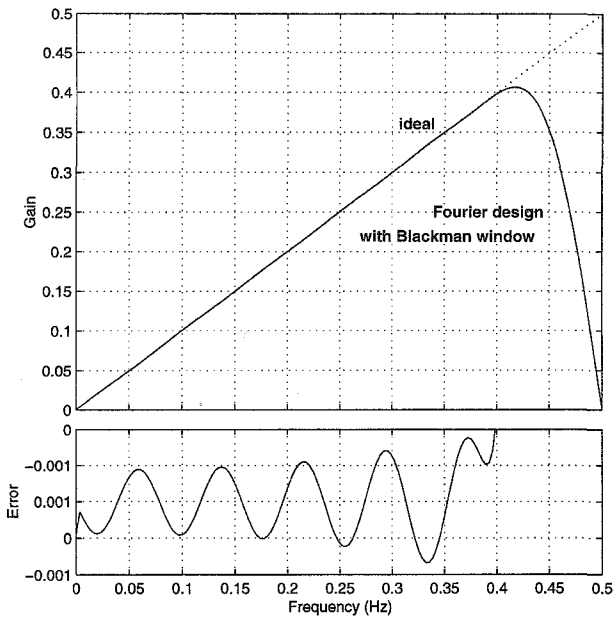

FIGURE 4. Reduction of Gibbs' phenomenon using window functions.

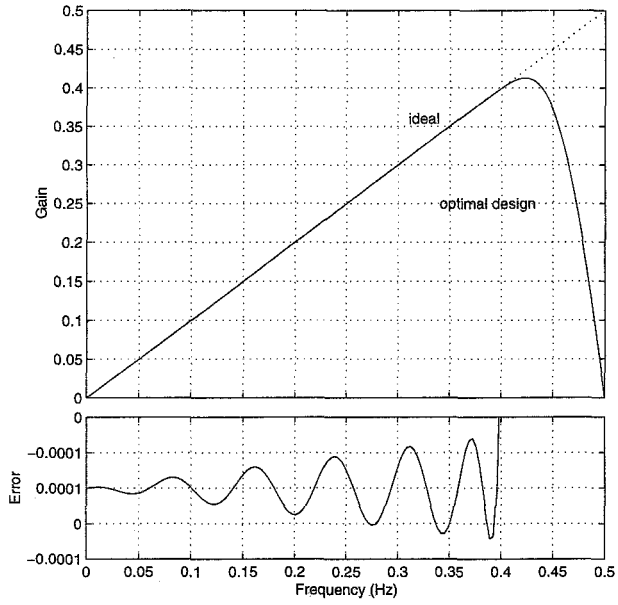

FIGURE 5. Amplitude response of the Remez 25th-order differentiator.

Clearly, this filter offers a better approximation to the ideal case over the whole frequency band than any presented previously. In turn, this provides a good solution for conditions of unknown or high dynamics.

1.6. Numerical designs

As mentioned in Section 1.3, better approximations of the ideal differentiator can be obtained from Taylor Series by using a higher order expansion. This is a subset of the filter design problem commonly referred to as numerical design. Consider a filter design based conceptually on a central difference formula derived from a 25th order Taylor series expansion of the derivative. Figure 6 shows the amplitude response of this filter and its deviation from ideal. The figure clearly demonstrates that a higher order Taylor series approximation better represents the ideal case over a wider bandwidth.

It is interesting to note that although the amplitude response of this filter over the whole spectrum is not as good as the one designed using an optimal approach, it is very good in the low-frequency band. As we will see in Sections 3 and 4, this makes it especially well suited for cases where the signal is primarily low-frequency in nature (like static surveys and airborne gravity).

1.7. Curve fitting for differentiation

An intuitive approach to estimating the derivative of a noisy discrete-time signal is by fitting a curve to it and then differentiating the curve fit. For purposes of illustration, consider using a least-squares approach to determine a polynomial that best fits the data and that can then be differentiated. As well as providing an estimate of the derivative, this will offer a certain level of smoothing that, depending on the situation, may or may not be desirable. The amount of smoothing will be a function of the order of the polynomial and the length of the sliding window in which the data are being fit. Other base functions such as splines may also be used for the curve fit.

Let the discrete-time signal at time instant t_k be given by f_k and let the sliding window of length (W+1) be centered around time t_k and index it such that the index i varies from $-W/2$ to W/2. Within this window, the best fit polynomial of order M therefore has the form

$$P(i) = a_0 + a_1 i + a_2 i^2 \ldots + a_M i^M \tag{10}$$

and its first derivative is given by

$$\frac{dP(i)}{dt} = a_1 + 2a_2 i + \ldots + Ma_M i^{M-1} \tag{11}$$

The polynomial coefficients in the above equations can be solved for using the standard unweighted least-squares solution equation

$$\mathbf{a} = (\mathbf{A}^T\mathbf{A})^{-1}\mathbf{A}^T\mathbf{f} \tag{12}$$

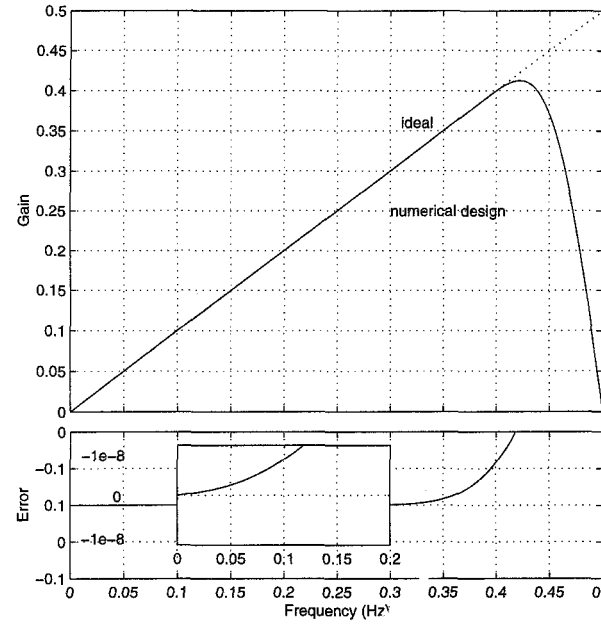

FIGURE 6. The amplitude response of a 25th-order numerical differentiating filter.

where $\mathbf{a} = [a_0 \ a_1 \ \ldots \ a_M]^T$ and the i^{th} row of $\mathbf{A}$ and $\mathbf{f}$ are given by

$$\mathbf{A}_i = \left[\frac{dP}{da_0}\frac{dP}{da_1}\cdots\frac{dP}{da_M}\right]_i \Bigg|_{i=-\frac{W}{2},\frac{W}{2}} \qquad \mathbf{f}_i = [f_{k-1}] \tag{13}$$

Performing this type of adjustment for every data point is computationally very burdensome. This can be remedied by making two major simplifications. First, because the term $(\mathbf{A}^T\mathbf{A})^{-1}\mathbf{A}^T$ in Eq. (12) is independent of the signal f, it only needs to be calculated once. Second, by setting $i = 0$, the expression for the value of the derivative in Eq. (11) at the center point of the window ($t=t_k$) is given by

$$\frac{dP(0)}{dt} = a_1 \tag{14}$$

Thus, only one coefficient is needed for each derivative to be calculated. This means that for the first derivative, only the second row of the term $(\mathbf{A}^T\mathbf{A})^{-1}\mathbf{A}^T$ is needed. The solution for the value of the function reduces to a convolution. If the second row of the above matrix is given by $\mathbf{h}$, then the first derivative of the function is given by

$$\frac{df_k}{dt} \approx \frac{dP(0)}{dt} = \sum_{i=-W/2}^{W/2} h_i f_{k+i} \tag{15}$$

This approach to fitting polynomials to a data set using least squares is referred to as Savitzky-Golay smoothing [see, e.g., Press et al., 1992 (p. 650–655)].

These curve-fitting filters will have symmetric impulse responses and will therefore have linear phase response causing only a constant time delay. When formulated as in Eq. (15), least-squares fitting of polynomials to a discrete time signal can be seen as applying an FIR filter. The least-squares adjustment becomes a filter design. This approach allows one to quantify the amount of smoothing that a best-fitting polynomial offers as a function of both the order of the polynomial M and the size of the sliding window (W+1).

It is important to realize how this type of filtering differs from optimal FIR filtering (as seen in Section 1.5). Although both might use a least-squares fit, they are fundamentally different. A filter designed using a curve-fit approach uses least squares to fit a curve to the data being operated on. It will have a corresponding frequency response. On the other hand, optimal design techniques use a least-squares fit to specify the desired frequency response.

Figure 7 shows the amplitude response of five polynomial fits. They are a set of 5th-order polynomials (M=5) designed with window lengths W= 101, 49, 25, 15, and 7. Also shown for comparison is the amplitude response of the ideal differentiator. Notice first that each offers a reasonably good approximation of the ideal case at low frequencies. The frequency range over which they do a good job of approximating the ideal differentiator is clearly a function of the length of the window. Intuitively this makes sense: If the sliding window is short, then higher-frequency information will be identified, whereas if it is large, only the low-frequency information will be preserved.

A frequency domain analysis allows one to quantify the amount of differentiation and smoothing being done by a polynomial fit. For example, imagine using a polynomial with M=5 and W=15 to differentiate a signal. Figure 7 shows that a good estimate of the derivative will be obtained for information up to approximately 0.08 Hz. Above that frequency, the information content will be attenuated. The first zero of this filter is at 0.19 Hz, and there are four more rises in the response as frequency increases. This characteristic can be useful or disastrous, depending on the signal being differentiated. This filter should only be applied if one is interested in the derivative of the information below 0.08 Hz. If there is any information content above 0.08 Hz that

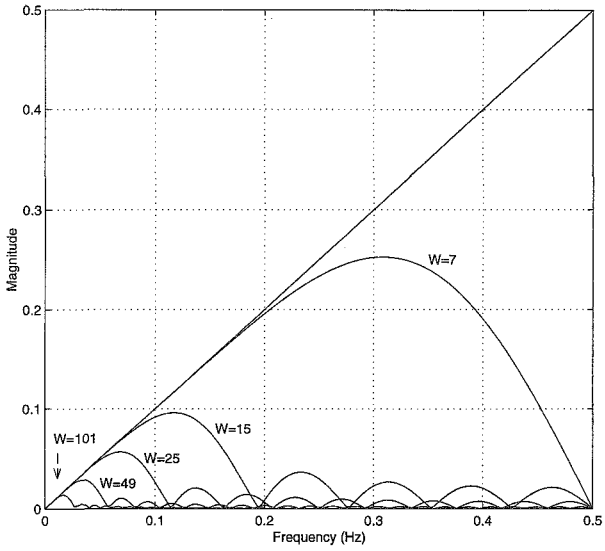

FIGURE 7. Amplitude responses of 5th-order polynomial fits as a function of filter length W.

cannot be considered noise, then the output of the filter will give a very poor and perhaps unacceptable estimate.

The behavior of a polynomial fit is also a function of the order of the polynomial. Figure 8 shows a plot of the *maximum undistorted frequency* (MUF) as a function of window length for polynomial orders M = 2, 3, 5, 10, and 20. (MUF is defined as the frequency above which the filter no longer approximates an ideal differentiator with more than 0.5% of the maximum frequency content of the signal.) This figure can be used to determine the range of parameters that are suitable for a given application. Obviously, a polynomial fit can only be used to estimate the derivative in cases where the signals are band-limited and low frequency in nature. The range of applicability is a function of the parameters M and W as given by Figure 8.

Because the curve fitting problem has been treated by using polynomial fitting as an example, some comments about other fits might be in order. Whether the curve being fit is a polynomial, parabola, or cubic spline, its frequency response will be similar in nature to those in Figure 7; it will be suitable for band-limited, low-frequency signals, and it will only approximate the ideal differentiator up to a certain frequency. In turn, this means that they can be used only for low dynamic or static conditions. This has been confirmed in the following investigations. Fenton and Townsend (1994) used a parabolic fit within the receiver to estimate the derivative. They found that velocity results were improved in static cases. Both Cannon et al. (1997) and Hebert (1997) approached this task in post mission using simulated GPS data by differentiating cubic spline fits. In each of these cases, good solutions were observed in static and low dynamic cases, but errors increased with higher dynamics.

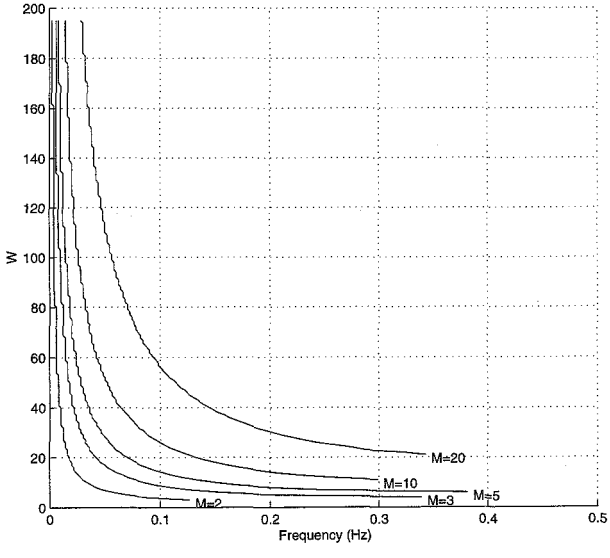

FIGURE 8. Maximum undistorted frequency as a function of window length for polynomial orders M = 2, 3, 5, 10, and 20.

1.8. Comments on other differentiation techniques

By restricting this discussion to the use of FIR filters, several other approaches have been ignored. For example, a Kalman filter smoother was studied in Hebert (1997). It is well known that a Kalman filter smoother will result in a smooth, band-limited solution. This result was confirmed in Hebert (1997). Because this approach has been shown to offer little or no improvement over the low-order Taylor series approximations, it will not be treated in this article.

2. METHODOLOGY

All of the differentiators treated in this article are FIR filters with linear phase. This means that they can be applied to any GPS data set using the discrete time convolution given by Eq. (2). Two software packages have been developed at the University of Calgary for this purpose: One is a preprocessor for differentiation in the measurement domain, and one is a postprocessor for differentiation in the position and velocity domains.

For the measurement domain investigations that are carried out in Section 3, the preprocessor called DER_DOP (DERived DOPpler) was written to apply any impulse response to the phase measurements according to Eq. (2). It derives a Doppler by differentiating the carrier phase data. A phase velocity trend method was used to detect cycle slips using the raw Doppler observable, and the filter was reset if gaps in the data or cycle slips were detected. In cases when the filter was reset, a central difference approximation was used to estimate the Doppler. This corresponds to a period that is half of the order of the filter each time the filter is reset. Each satellite is treated independently, meaning that a slip on one will not reset the filter for other satellites.

The data were then processed using an L1 float solution in the software package KINGSPAD (Kinematic Geodetic System for Position and Attitude Determination) developed at the University of Calgary.

For the position and velocity domain investigations that are carried out in Section 4, the postprocessor called GPSACC was used. It also applies any impulse

response according to Eq. (2). Any gaps in the time-tagged position and velocity solutions are filled in using a linear interpolation before filtering.

In the numerical studies, curve fits and Fourier series techniques are not used. As discussed previously, their range of applicability is severely limited.

3. MEASUREMENT DOMAIN ANALYSES (DERIVED DOPPLER)

To analyze the performance of the different methods of differentiation in the measurement domain, three test data sets are analyzed: first, a static data set on a 6-m baseline; second, four flight lines from an airborne gravimetry test conducted by the University of Calgary are examined; finally, the results of a test on an Anorad precision motion table are presented. All three data sets were collected using a 1-Hz GPS sampling frequency.

3.1. No dynamic case: static data analysis

For the static case, data were collected on a baseline of approximately 6 m with an Ashtech Z-XII and a Trimble 4000SSE receiver. Approximately 40 minutes of data were collected for the analysis. After a static initialization period of 100 s, the rest of the data were processed in kinematic mode. The errors in velocity obtained by deriving a Doppler using the 1st- and 3rd-order Taylor series approximations and 49th-order differentiators designed using numerical and optimal approaches are displayed in Table 1. Also shown are the results obtained if the receiver-generated raw Doppler is used.

Table 1 shows that each method of phase differentiation provides significantly better results than the raw Doppler in both root-mean-square (RMS) and mean values for all three direction components. The best RMS improvement is realized using the first-order Taylor series approximation, followed by the third-order and the numerical filters. The optimal differentiator gives the poorest results, but this is expected. Because the data set is static, there is no velocity information in the frequency bands where the Taylor series approximations begin to deviate from the ideal differentiator. Therefore, instead of causing differentiation errors in this band, the two approximations actually behave similarly to low-pass filters and dampen some of the higher frequency noise. However, because the numerical and optimal differentiators are still close to ideal in the higher band, they tend to amplify the noise. This effect is shown in Figure 9, where the frequency spectrum of the residuals for the first-order and optimal differentiators for the north direction are displayed.

TABLE 1

GPS velocity errors for static data

	RMS (mm/s)			Mean (mm/s)		
Doppler type	*N*	*E*	*U*	*N*	*E*	*U*
Raw	4.00	3.11	7.04	0.20	−1.32	1.75
1st order	0.65	0.48	1.00	0.20	−0.05	0.18
3rd order	0.93	0.70	1.54	0.21	−0.07	0.17
Numerical (49)	1.24	0.96	2.16	0.20	−0.05	0.17
Optimal (49)	1.33	1.04	2.32	0.20	−0.05	0.18

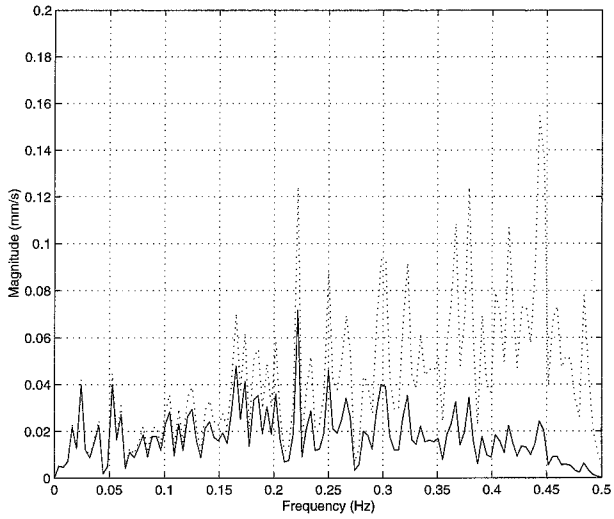

FIGURE 9. Spectrum of residuals for first-order and Remez (dotted line) differentiators, North direction, static data.

It is also important to notice that the numerical differentiator offers a better solution than the optimal differentiator for static cases. This can be explained by looking at Figures 5 and 6. The error in the response of the numerical filter at very low frequencies is on the order of 1×10^{-8}, whereas it is on the order of 1×10^{-5} for the optimal filter.

3.2. Low dynamic case: airborne gravimetry testing

Airborne gravimetry is an emerging technology that provides a powerful tool for both geodesy and geophysical exploration. Using airborne techniques, detailed local and regional gravity field information can be collected in a rapid and cost-effective manner. In addition,

areas that are inaccessible to terrestrial gravity survey methods can now be surveyed with relative ease. It is an important case study because it is a low-frequency dynamic test and provides an excellent example of an application where accurate estimates of platform acceleration are required.

3.2.1. The Importance of GPS in airborne gravity

The principle of airborne gravity is the differencing of measurements from two subsystems—one that contains the effect of the gravity field, and one that does not. The prototype system developed at the University of Calgary consists of a strapdown inertial navigation system (INS), differential GPS (DGPS) combination (see Wei & Schwarz, 1998). The accelerometers of the INS measure specific force, which is the combined acceleration caused by aircraft motion and the reaction force from the gravity field of the earth. DGPS provides highly accurate position and velocity information, which when differentiated provide a measure of aircraft acceleration. Therefore, by differencing the output of the two systems, an estimate of the gravity field of the earth, contaminated by measurement noise, is obtained. The accuracy of the determined gravity field information is directly related to the errors in the DGPS-derived accelerations. Therefore, a study of airborne gravity results provides a means of comparing derived Doppler velocity results. The dominant errors in DGPS acceleration are short-term errors caused mainly by measurement noise. Figure 10 shows a typical error spectrum for GPS-determined accelerations using actual flight data (1 mGal = 0.00001 m/s^2). The figure assumes a flight velocity of 80 m/s and a flight height of 2.5 km.

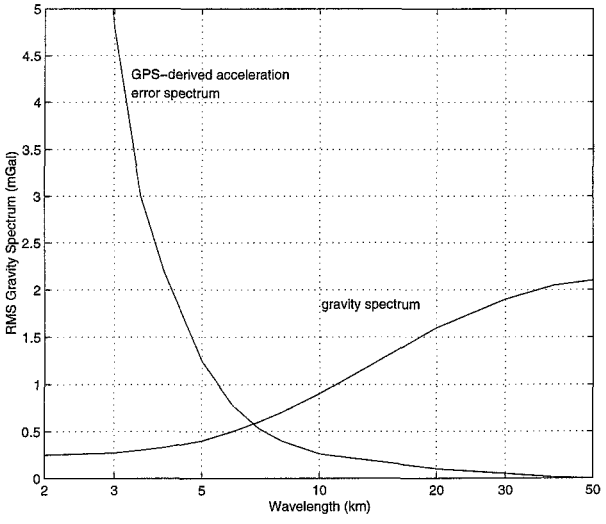

FIGURE 10. Influence of GPS acceleration errors on minimum resolvable gravity wavelength. (Schwarz and Li, 1996).

3.2.2. Airborne data analysis

To analyze the improvement in airborne gravity results when the acceleration is estimated from derived Doppler GPS velocity, four flight lines of approximately 1000-s duration from an airborne gravity test are analyzed. The test took place in September 1996 over the Rocky Mountains in Alberta, Canada. Trimble 4000SSI receivers were used for both the master and remote stations. More details of this test can be found in Glennie and Schwarz (1998). The onboard strapdown INS/DGPS combination is used to derive gravity disturbances. The estimated gravity disturbances are then compared with reference gravity disturbances upward continued from ground gravity measurements. The accuracy of the upward continued reference is approximately 1.5–2.0 mGal (Schwarz and Glennie, 1997). The accuracy of the determined gravity disturbances is then a function of GPS and INS errors. Because the INS errors are dominant at lower frequencies (or higher averaging time, e.g., above 60 s), the accuracy of the determined disturbances are mainly a function of GPS noise. Tables 2–5 give the errors in gravity disturbance estimation for different GPS Doppler acceleration determinations and for different filtering periods. The optimal and numerical differentiators are each 49th-order filters. The 30-, 60-, and 90-s filtering times are typical periods used in airborne gravity.

An analysis of the results in the above four tables shows that the first-order filter now performs worse than the raw Doppler observations. The reason for the change in performance when compared with the static

TABLE 2

Flight line 1 gravity disturbance estimation errors (RMS in mGal)

Doppler type	15 s	30 s	60 s	90 s
Raw	69.6	18.7	6.8	4.0
1st order	170.1	27.0	4.5	3.5
3rd order	54.5	15.0	4.0	3.4
Numerical (49)	54.5	15.0	4.0	3.4
Optimal (49)	54.6	15.0	4.1	3.4

TABLE 3

Flight line 2 gravity disturbance estimation errors (RMS in mGal)

Doppler type	*15 s*	*30 s*	*60 s*	*90 s*
Raw	53.0	15.0	4.3	3.7
1st order	133.7	18.6	4.3	3.5
3rd order	36.1	9.4	4.1	3.5
Numerical (49)	36.1	9.4	4.1	3.5
Optimal (49)	36.1	9.4	4.1	3.5

TABLE 5

Flight line 4 gravity disturbance estimation errors (RMS in mGal)

Doppler type	*15 s*	*30 s*	*60 s*	*90 s*
Raw	53.0	13.2	4.5	2.5
1st order	128.1	16.5	3.4	2.3
3rd order	38.6	9.5	3.4	2.3
Numerical (49)	38.6	9.5	3.4	2.3
Optimal (49)	38.6	9.5	3.4	2.3

results is because of the introduction of vehicle dynamics into the data set. A spectrum of the up-velocity for the airborne test, given in Figure 11, clearly shows that there is velocity information up to approximately 0.2 Hz. The remaining spectrum above 0.2 Hz is due mostly to measurement noise. Recall Figure 1 that shows the amplitude response of the first- and third-order differentiators. The first-order response deviates significantly from ideal in the band from 0.02 to 0.2 Hz. This deviation is in a band where vehicle velocity is present and explains why poor results were obtained from the first-order differentiator. The third-order differentiator, however, is still very close to ideal up to 0.2 Hz, and therefore shows good results that are identical to the numerical and optimal results.

3.3. High dynamic case: motion table data analysis

As a final method of comparison of differentiation techniques in the measurement domain, a data set collected on an Anorad precision motion table was analyzed. An Ashtech Z-XII antenna was placed on the motion table and followed a prescribed sinusoidal trajectory. A second Ashtech Z-XII was used and approximately 20 min of data were collected in differential mode. The Anorad table allows the user to specify a trajectory along one axis and provides a position and velocity reference for the motion at the submillimeter (millimeters per second) level. The table therefore allowed the generation of a high dynamic data set with a very accurate reference. A spectrum of the reference velocities given by the table for the test is shown in Figure 12 to give an idea of the test dynamics. The results of the analysis are given in Table 6. The optimal and numerical differentiators are again 49th-order filters.

The results presented in Table 6 show that for this high dynamic data set, the optimal and numerical differentiators perform significantly better than the two

TABLE 4

Flight line 3 gravity disturbance estimation errors (RMS in mGal)

Doppler type	*15 s*	*30 s*	*60 s*	*90 s*
Raw	52.6	13.5	4.0	2.4
1st order	146.9	19.2	3.2	1.8
3rd order	38.2	9.9	2.8	1.8
Numerical (49)	38.1	9.9	2.8	1.8
Optimal (49)	38.2	9.9	2.8	1.8

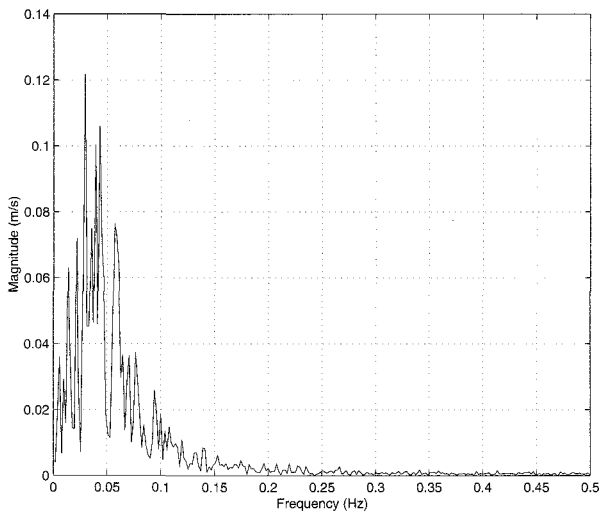

FIGURE 11. Spectrum of up velocity for airborne gravity data.

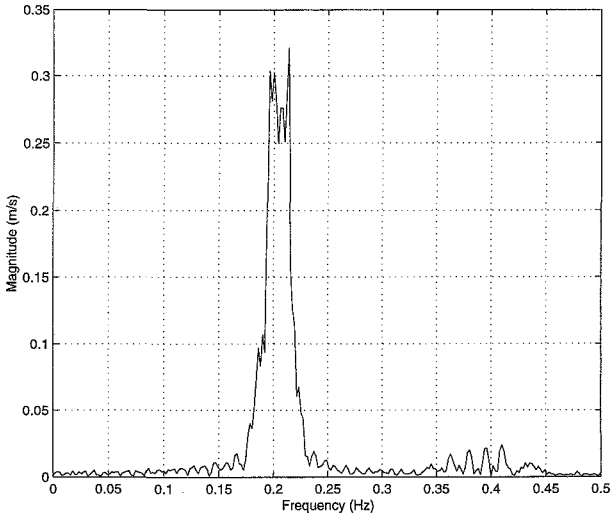

FIGURE 12. Spectrum of reference velocities for Anorad table test.

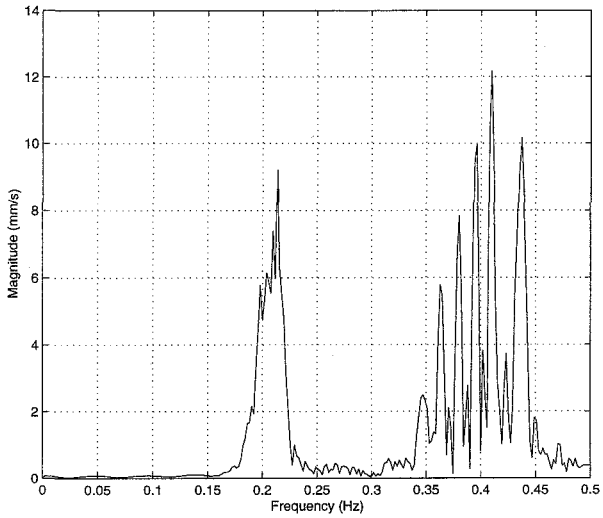

FIGURE 13. Spectrum of the difference between the third-order and Remez solutions.

Taylor series approximations. This is obviously because of the presence of the higher frequency velocity information at 0.15–0.25 Hz and in the band around 0.4 Hz. In these bands, the Taylor series approximations deviate significantly from the ideal differentiator, and therefore do a poor job of estimating the higher dynamic velocities. Because the optimal and numerical differentiators have near ideal responses up to 0.4 Hz, they have no problem properly differentiating the higher frequency dynamics. Figure 13 gives a plot of the difference in the residuals between the third-order approximation and the optimal differentiator. The plot clearly shows that the errors in the third-order derivative grow with frequency.

The optimal differentiator outperforms the numerical one in this case because it is by nature designed to have a better response over the whole spectrum. This might not be the case if the motion had more low-frequency content.

TABLE 6

GPS velocity errors for Anorad test in the measurement domain

Doppler type	*RMS (mm/s)*	*Mean (mm/s)*
Raw	261.9	−2.5
1st order	237.1	−1.2
3rd order	48.9	−0.5
Numerical (49)	27.3	−0.5
Optimal (49)	27.0	−0.5

4. POSITION AND VELOCITY DOMAIN ANALYSES

To analyze the performance of the different methods of differentiation in the position and velocity domains, two tests were conducted. In both, the output of the GPS engine KINGSPAD was used as input to the post-processor GPS Acceleration (GPSACC). In the first case, the low dynamic airborne gravity case was studied. In the second, the higher dynamic case study provided by the precision motion table results was used again.

4.1. Low dynamic case: airborne gravimetry testing

In this case, the position of the aircraft was determined using KINGSPAD and then differentiated twice using each filter to obtain acceleration. The same flight lines that were used in Section 3.2 are again used. The same independent upward continued reference is also used for the evaluation. The results are shown in Tables 7–10.

The best results were again found to be at a filtering period of 90 s and agree with those obtained by differentiating in the measurement domain. It is important to notice that as the frequency band becomes larger (i.e., at filtering periods of 15, 30, and 60 s), the acceleration results achieved by differentiation in the position domain were better than those achieved by differentiation in the measurement domain. This can be seen by comparing Tables 2–5 with Tables 7–10. This may become

TABLE 7

Flight line 1 gravity disturbance estimation errors (RMS in mGal)

Differentiation	*15 s*	*30 s*	*60 s*	*90 s*
1st order	298.8	43.3	5.0	3.6
3rd order	47.4	14.8	3.9	3.5
Numerical (25)	47.3	14.8	3.9	3.5
Optimal (25)	47.1	14.9	4.0	3.5

TABLE 8

Flight line 2 gravity disturbance estimation errors (RMS in mGal)

Differentiation	*15 s*	*30 s*	*60 s*	*90 s*
1st order	251.8	30.7	4.2	3.3
3rd order	27.0	7.6	3.7	3.3
Numerical (25)	27.0	7.6	3.7	3.3
Optimal (25)	27.0	7.5	3.7	3.3

TABLE 9

Flight line 3 gravity disturbance estimation errors (RMS in mGal)

Differentiation	*15 s*	*30 s*	*60 s*	*90 s*
1st order	283.5	41.5	3.6	1.9
3rd order	33.0	8.9	2.6	1.9
Numerical (25)	33.0	8.9	2.6	1.9
Optimal (25)	33.1	9.0	2.6	1.9

TABLE 10

Flight line 4 gravity disturbance estimation errors (RMS in mGal)

Differentiation	*15 s*	*30 s*	*60 s*	*90 s*
1st order	258.2	29.1	3.6	2.4
3rd order	33.3	9.2	3.3	2.4
Numerical (25)	33.3	9.2	3.3	2.4
Optimal (25)	33.0	9.1	3.3	2.4

increasingly important as the resolution of airborne gravity systems is increased.

Numerical and optimal filters with 49th-order were also tried and found to offer no improvement over the 25th-order filters.

4.2. High dynamic case: motion table data analysis

In this case, the position of the antenna on the motion table was determined using KINGSPAD and then differentiated using a number of filters to obtain velocity. This was then compared with the truth offered by the table.

Several observations can be made from Table 11. The first one is that the Taylor series approximations offer considerably worse solutions than the numerical and optimal filters. Looking at their filter responses (Figure 1) and the spectrum of the motion of the table (Figure 12), this is obviously because they are far from ideal in the part of the spectrum corresponding to the motion of the table. Second, notice that the 49th-order numerical and optimal filters offer better solutions than the 25th-order ones. Finally, notice that in all cases, the optimal filter offers a better solution than the numerical filter. Higher order optimal filters were tried and did not improve the solution.

It is also important to notice that the level of accuracy achieved in Section 3.3 with measurement domain techniques is greater than that achieved with these position domain techniques. This is because when the dynamics are high, input to the GPS engine must be as accurate as possible. This is only true if differentiation is done in the measurement domain.

CONCLUSIONS AND RECOMMENDATIONS FOR FUTURE WORK

A number of filters of varying complexity were studied. They were characterized in the frequency domain to allow an assessment of their applicability in different dynamic scenarios. Low-order Taylor series and curve fits were shown to be useful only in cases of very low dynamics, and dangerous otherwise. Both offer distortion above some band of applicability. Although there are situations where these types of filters might be useful, extreme care is advised if they are going to be used in general cases. For cases where the dynamics are very low, however, it was shown that differentiators designed using the numerical approach offer the best response.

TABLE 11

GPS velocity errors for Anorad test in the position domain

Differentiation	*RMS (mm/s)*	*Mean (mm/s)*
1st order	240.7	0.6
3rd order	48.4	0.6
Numerical (25)	34.1	0.6
Optimal (25)	31.1	0.6
Numerical (49)	31.6	0.6
Optima (49)	31.0	0.5

Differentiators designed using the Fourier series offer good approximations to the ideal case if a window function is used. They offer a better response than Taylor series designs and polynomial fits over the whole frequency band. Their use, however, is limited by the need to keep the error in the response low for high orders. The response of filters designed using an optimal approach was shown to offer the same range of applicability as the Fourier designs, but better responses for the same order.

To compare methods of computing a derived Doppler for GPS velocity and acceleration determination, three data sets with varying degrees of dynamics were analyzed. Based on this analysis, the following conclusions can be drawn.

- Deriving Doppler from the raw phase measurements provides accurate estimates of vehicle velocity, as long as the differentiator applied is close to ideal in the frequency band where the vehicle velocity is present.
- The optimal differentiator provides the best results for high dynamics because it most closely approximates the ideal differentiator throughout the frequency band of interest.
- The Taylor series approximations provide reasonable results only for cases of low-frequency motion. This is due to their deviation from an ideal differentiator in the middle of the frequency band. Caution should be exercised when trying to apply these differentiation techniques.

To compare the results by differentiation in the measurement domain with those in the position domain, the low and higher frequency cases were repeated. Based on this analysis, the following conclusions can be drawn.

- In the low dynamic case of airborne gravity, differentiation in the position domain appears to give better results than in the measurement domain.
- For the high dynamic case of the precision motion table, differentiation in the measurement domain gives better results than in the position domain.

Future work in estimating accurate velocity and acceleration from GPS measurements might include:

- Designing a lowpass differentiating filter after a careful analysis of the spectral content of the vehicle velocity signal. For example, for the airborne gravity flight, the signal above 0.2 Hz is mostly measurement noise. Therefore, an optimal differentiator might be designed with a cutoff frequency of 0.2 Hz instead of 0.4 Hz.
- Applying a noise reduction technique such as Kalman filtering/smoothing or spline fitting to remove noise after the phase measurements have been differentiated.
- Combining multiple master-remote station combinations as in (Bruton, 1998) or (Raquet and Lachapelle, 1997).
- Evaluating the appropriateness and possible advantages of using infinite impulse response differentiating filters. ■

REFERENCES

Antoniou, A. (1993). Digital filters: Analysis, design and applications (689 pp.), New York: McGraw-Hill.

Brozena, J.M., Mader G.L., & Peters M.F. (1989). Interferometric global positioning system: Three-dimensional positioning source for airborne gravimetry. J. Geophys. Res., 94, 12153–12162.

Bruton, A.M. (1998). Kinematic positioning using adaptive filters and multiple DGPS receiver configurations. In Advances in positioning and reference frames: IAG International Symposium no. 118, Rio De Janeiro, Brazil, September 3–9, 1997 (pp. 325–330). Berlin, Heidelberg: Springer-Verlag.

Cannon, M.E., Lachapelle, G., Szarmes, M.C., Hebert, J.M., Keith, J., & Jokerst S. (1997). DGPS kinematic carrier phase signal simulation analysis for precise velocity and position determination. J. Inst. Navig., 44, 231–245.

Cheney, W., & Kincaid, D. (1994). Numerical methods and computing, 3rd Edition (578 pp.). Pacific Grove, California: Brooks/Cole Publishing.

Fenton, P., & Townsend, B. (1994). NovAtel Communications Ltd. What's new? In Proceedings of International Symposium on Kinematic Systems in Geodesy, Geomatics and Navigation

(KIS94) (pp. 25–29), Banff, Canada: The Department of Geomatics Engineering, The University of Calgary.

Glennie, C., & Schwarz K.P. (1998). A comparison and analysis of airborne gravimetry results from two strapdown inertial/DGPS systems. Submitted to J. Geodesy, 1998.

Hammada,Y. (1996). Airborne gravimetry by GPS/INS: A comparison of filtering methods, M.Sc. Thesis (111 pp.), Calgary: Department of Geomatics Engineering, University of Calgary.

Hebert, J. (1997). High accuracy GPS velocity using the carrier phase observable. In Proceedings of International Symposium on Kinematic Systems in Geodesy, Geomatics and Navigation (KIS97) (pp. 265–269), Banff, Canada: The Department of Geomatics Engineering, The University of Calgary.

Orfanidis, S.J. (1996). Introduction to signal processing (798 pp.), Toronto: Prentice Hall Signal Processing Series.

Press, W.H., Teukolsky, S.A, Vetterling, W.T., & Flannery B.P. (1992). Numerical recipes in C, 2nd Edition (994 pp.), New York: Cambridge University Press.

Raquet, J., & Lachapelle, G. (1997). Long distance kinematic carrier-phase ambiguity resolution using a simulated reference receiver network. In Proceedings ION GPS–97 (pp. 1747–1756), Alexandria, VA: The Institute of Navigation.

Schwarz K.P., & Glennie, C. (1997). Improving accuracy and reliability of airborne gravimetry by multiple sensor configurations. In Geodesy on the move: IAG International Symposium no. 119: Rio De Janeiro, Brazil, September 3–9, 1997, (pp. 11–17). Berlin, Heidelberg: Springer-Verlag.

Schwarz, K.P., & Z. Li. (1996). An introduction to airborne gravimetry and its boundary value problems, IAG International Summer School, Como, Italy, May 26–June 7.

Skaloud, J., & Schwarz, K.P. (1998). Accurate orientation for airborne mapping systems. In Proceedings of the International Society for Photogrammetry and Remote Sensing (ISPRS)—Commission I, real-time mobile technologies, Cambridge, UK, July 13–17. (Also submitted to J. Photogram. Remote Sensing).

Van Dierendonck, K.J., Cannon, M.E., Wei, M., & Schwarz, K.P. (1994). Error sources in GPS-derived acceleration for airborne gravimetry. In Proceedings of ION National Technical Meeting (pp. 811–820), San Diego: The Institute of Navigation.

Wei, M., Ferguson, S., & Schwarz, K.P. (1991). Accuracy of GPS-derived acceleration from moving platform tests. In Proceedings of IAG Symposium 110, From Mars to Greenland: Charting gravity with space and airborne instruments (pp. 235–249), New York: Springer-Verlag.

Wei, M., & Schwarz K.P. (1998). Flight test results from a strapdown airborne gravity system. J. Geodesy, 72, 323–332.

BIOGRAPHIES

Alex Bruton is a Ph.D. student in the Department of Geomatics Engineering at the University of Calgary and holds a B.Sc. in Surveying Engineering from the same university. His research interests include integrated navigation systems, advanced filtering methods, and airborne gravimetry.

Craig Glennie is a Ph.D. student in the Department of Geomatics Engineering at the University of Calgary. He holds a B. Sc. in Geomatics Engineering from the same university. Currently, his research interests include the use of multisensor systems for precise positioning, attitude determination, and airborne gravimetry.

Dr. Klaus-Peter Schwarz is a professor in the Department of Geomatics Engineering at the University of Calgary and President of the International Association of Geodesy. He holds degrees from universities in Germany, Canada, and Austria, and an honorary degree from China. He is also a member of the Russian Academy of Navigation and Motion Control. His area of expertise is geodesy with special emphasis on the use of inertial systems in geomatics and the integration of satellite and inertial techniques for precise aircraft positioning, attitude determination, and gravity field modeling.

Peer Review: This article has been peer-reviewed and accepted for publication according to the guidelines provided in the Information for Contributors.